Cluster formation and anomalous fundamental diagram in an ant-trail model

Katsuhiro Nishinari*
Institut für Theoretische Physik, Universität zu Köln, D-50937 Köln, Germany

Debashish Chowdhury†
Department of Physics, Indian Institute of Technology, Kanpur 208016, India

Andreas Schadschneider‡
Institut für Theoretische Physik, Universität zu Köln, D-50937 Köln, Germany
(Received 29 November 2002; published 28 March 2003)

A recently proposed stochastic cellular automaton model [J. Phys. A 35, L573 (2002)], motivated by the motions of ants in a trail, is investigated in detail in this paper. The flux of ants in this model is sensitive to the probability of evaporation of pheromone, and the average speed of the ants varies nonmonotonically with their density. This remarkable property is analyzed here using phenomenological and microscopic approximations thereby elucidating the nature of the spatiotemporal organization of the ants. We find that the observations can be understood by the formation of loose clusters, i.e., space regions of enhanced, but not maximal, density.

DOI: 10.1103/PhysRevE.67.036120 PACS number(s): 02.50.Ey, 05.40.−a

I. INTRODUCTION

Particle-hopping models have been used widely in the recent years to study the spatiotemporal organization in systems of interacting particles driven far from equilibrium [1–6]. Often such models are formulated in terms of cellular automata (CA) [7]. Examples of such systems include vehicular traffic [8–11] where the vehicles are represented by particles, while their mutual influence is captured by the interparticle interactions. Usually, these interparticle interactions tend to hinder their motions so that the *average speed* decreases *monotonically* with the increasing density of the particles. In the usual form of the fundamental diagram, i.e., the flux-density relation, this nonmonotonicity corresponds to the existence of an inflection point. In a recent paper [12], we have reported a counter example, motivated by the flux of ants in a trail [13], where, the average speed of the particles varies nonmonotonically with their density because of the coupling of their dynamics with another dynamical variable. In Ref. [12] we presented numerical evidence in support of this unusual feature of the model and indicated the physical origin of this behavior in terms of a heuristic mean-field argument. In this paper, we present the corresponding detailed *analytical* calculations, together with further numerical results, that provide deep insight into the model.

The paper is organized as follows: The ant-trail model [12] is defined in Sec. II and compared with some closely related models in Sec. III. Section IV presents results obtained from a microscopic cluster approximation. Although this approach does not reproduce the observed sharp cross-over it will help us to get a better understanding of the microscopic structure of the stationary state. A heuristic homogeneous mean-field theory, which was sketched briefly in Ref. [12], is presented in detail in Sec. V. This theory produces better results than the cluster approximation. However, it accounts only for the *qualitative* features of the fundamental diagram obtained by computer simulations. Therefore, in Sec. VI, we present a different approach that leads to the main results. In this section, we have computed some quantities that provide information as to the state of occupation of the site immediately in front of an ant. These quantities not only help us in identifying *three* regimes of density, with corresponding characteristic features, but also provide insights that we exploit in developing a different scheme for analytical calculations. The results of this different scheme, that we call ''loose-cluster approximation'' (for reasons which will be clear in Sec. VI), are in reasonably good *quantitative* agreement with the data obtained from computer simulations. The effects of replacing the parallel updating by random sequential updating is explored in Sec. VII. The results are summarized and conclusions are drawn in Sec. VIII. In two Appendices some details of the calculations for the cluster-theoretic approaches are given.

II. THE ANT-TRAIL MODEL

The ants communicate with each other by dropping a chemical (generically called *pheromone*) on the substrate as they crawl forward [14–16]. Although we cannot smell it, the trail pheromone sticks to the substrate long enough for the other following sniffing ants to pick up its smell and follow the trail. Ant trails may serve different purposes (trunk trails, migratory routes) and may also be used in a different way by different species. Therefore, one-way trails are observed as well as trails with counterflow of ants.

In Ref. [12], we developed a particle-hopping model, formulated in terms of stochastic CA [7], which may be interpreted as a model of unidirectional flow in an ant trail. As in

*Permanent address: Department of Applied Mathematics and Informatics, Ryukoku University, Shiga, Japan (email address: knishi@rins.ryukoku.ac.jp). Electronic address: kn@thp.uni-koeln.de

†Electronic address: debch@iitk.ac.in

‡Electronic address: as@thp.uni-koeln.de

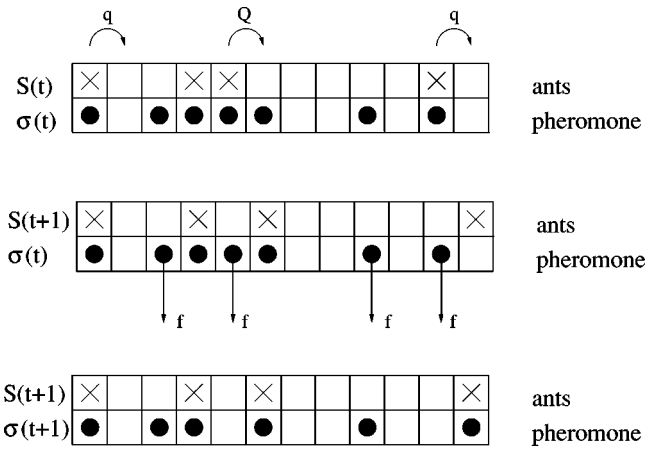

FIG. 1. Schematic representation of typical configurations; it also illustrates the update procedure. Top: configuration at time t, i.e., *before* stage *I* of the update. The nonvanishing hopping probabilities of the ants are also shown explicitly. Middle: configuration *after* one possible realization of *stage I*. Two ants have moved compared to the top part of the figure. Also indicated are the pheromones that may evaporate in stage II of the update scheme. Bottom: Configuration *after* one possible realization of *stage II*. Two pheromones have evaporated and one pheromone has been created due to the motion of an ant.

Ref. [12], rather than addressing the question of the emergence of the ant trail, we focus attention here on the traffic of ants on a trail which has already been formed. Furthermore, we have assumed unidirectional motion. The effects of counterflow, which are important for some species, will be investigated in the future. Each site of our one-dimensional ant-trail model represents a cell that can accomodate at most one ant at a time (see Fig. 1). The lattice sites are labeled by the index i ($i=1,2,\ldots,L$); L being the length of the lattice. We associate two binary variables S_i and σ_i with each site i, where S_i takes the value 0 or 1 depending on whether the cell is empty or occupied by an ant. Similarly, $\sigma_i=1$ if the cell i contains pheromone; otherwise, $\sigma_i=0$. Thus, we have two subsets of dynamical variables in this model, namely, $\{S(t)\}\equiv(S_1(t),S_2(t),\ldots,S_i(t),\ldots,S_L(t))$ and $\{\sigma(t)\}\equiv(\sigma_1(t),\sigma_2(t),\ldots,\sigma_i(t),\ldots,\sigma_L(t))$. The instantaneous state (i.e., the configuration) of the system at any time is specified completely by the set $(\{S\},\{\sigma\})$.

Since a unidirectional motion is assumed, ants do not move backward. Their forward-hopping probability is higher if it smells pheromone ahead of it. The state of the system is updated at each time step in *two stages*. In stage I, ants are allowed to move. Here the subset $\{S(t+1)\}$ at the time step $t+1$ is obtained using the full information $[\{S(t)\},\{\sigma(t)\}]$ at time t. Stage II corresponds to the evaporation of pheromone. Here only the subset $\{\sigma(t)\}$ is updated so that at the end of stage II, the new configuration $[\{S(t+1)\},\{\sigma(t+1)\}]$ at time $t+1$ is obtained. In each stage, the dynamical rules are applied *in parallel* to all ants and pheromones, respectively.

(a) Stage I: motion of ants. An ant in cell i that has an empty cell in front of it, i.e., $S_i(t)=1$ and $S_{i+1}(t)=0$, hops forward with

$$\text{probability}=\begin{cases} Q & \text{if } \sigma_{i+1}(t)=1, \\ q & \text{if } \sigma_{i+1}(t)=0, \end{cases} \tag{1}$$

where, to be consistent with real ant trails, we assume $q<Q$.

(b) Stage II: evaporation of pheromones. At each cell i occupied by an ant after stage I a pheromone will be created, i.e.,

$$\sigma_i(t+1)=1 \quad \text{if } S_i(t+1)=1. \tag{2}$$

On the other hand, any ''free'' pheromone at a site i not occupied by an ant will evaporate with the probability f per unit time, i.e., if $S_i(t+1)=0$, $\sigma_i(t)=1$, then

$$\sigma_i(t+1)=\begin{cases} 0 & \text{with probability } f, \\ 1 & \text{with probability } 1-f. \end{cases} \tag{3}$$

Note that the dynamics conserves the number N of ants, but not the number of pheromones.

The rules can be written in a compact form as the coupled equations

$$S_j(t+1)=S_j(t)+\min[\eta_{j-1}(t),S_{j-1}(t),1-S_j(t)] - \min[\eta_j(t),S_j(t),1-S_{j+1}(t)], \tag{4}$$

$$\sigma_j(t+1)=\max(S_j(t+1),\min[\sigma_j(t),\xi_j(t)]), \tag{5}$$

where ξ and η are stochastic variables defined by $\xi_j(t)=0$ with the probability f and $\xi_j(t)=1$ with $1-f$, and $\eta_j(t)=1$ with the probability $p=q+(Q-q)\sigma_{j+1}(t)$ and $\eta_j(t)=0$ with $1-p$. This representation is useful for the development of approximation schemes.

III. COMPARISON WITH OTHER MODELS

In this section, we compare the ant-trail model first with the Nagel-Schreckenberg (NS) model [17] to show that in various limits it reduces to the NS model with different hopping probabilities. This comparison also helps in formulating the task of our analytical calculation from alternative perspectives. We also compare the ant-trail model with some other models all of which share a common feature: the dynamics of the ''particles'' are coupled to another dynamical variable.

A. The Nagel-Schreckenberg model

The NS model [17] is the minimal particle-hopping model for vehicular traffic on freeways. In the general version of the NS model the particles, each of which represents a vehicle, can have a maximum speed of $V_{\max}$. However, by the term ''NS model'' in this paper, we shall always mean the NS model with $V_{\max}=1$, so that each particle can move forward, by one lattice spacing, with probability q_{NS} if the lattice site immediately in front is empty.

The most important quantity of interest in the context of flow properties of the traffic models is the *fundamental diagram*, i.e., the flux-versus-density relation, where flux is the product of the density and the average speed. For a hopping

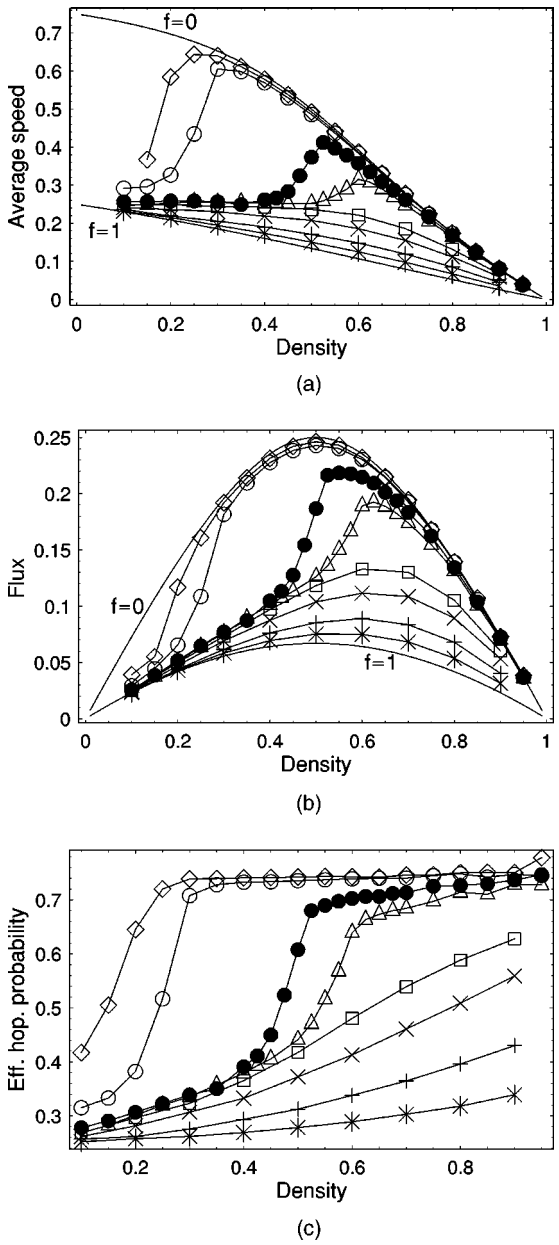

FIG. 2. The average speed (a), flux (b), and effective hopping probability (c) of the ants, extracted from computer simulation data, are plotted against their densities for the parameters $Q=0.75$, $q=0.25$. The discrete data points corresponding to $f=0.0005$ ($\diamond$), 0.001 ($\circ$), 0.005 ($\bullet$), 0.01 ($\triangle$), 0.05 ($\square$), 0.10 ($\times$), 0.25 ($+$), and 0.50 ($*$) have been obtained from computer simulations; the lines connecting these data points merely serve as the guide to the eye. In (a) and (b), the cases $f=0$ and $f=1$ are also displayed, which correspond to the NS model with $q_{\rm eff}=Q$ and q, respectively.

probability q_{NS} at a given density $\rho=N/L$, the exact flux $F(\rho)$ in the NS model is given by [8,18]

$$F_{NS}(\rho)=\frac{1}{2}[1-\sqrt{1-4q_{NS}\rho(1-\rho)}], \tag{6}$$

which reduces to $F_{NS}(\rho)=\min(\rho,1-\rho)$ in the deterministic limit $q_{NS}=1$.

Note that the expression (6) remains invariant under the interchange of ρ and $1-\rho$; this ''particle-hole'' symmetry of the NS model leads to a fundamental diagram that is symmetrical about $\rho=1/2$. In contrast, the fundamental diagrams of our ant-trail model [see Fig. 2(b)] do not possess this symmetry except in the special cases of $f=0$ and $f=1$. As explained in Ref. [12], in the two special cases $f=0$ and $f=1$ the ant-trail model becomes identical to the NS model with $q_{NS}=Q$ and $q_{NS}=q$, respectively, and, hence, recovers the particle-hole symmetry in these two special limits.

The flux F and the average speed V of vehicles are related by the hydrodynamic relation $F=\rho V$. The density dependence of the average speed in our ant-trail model is shown in Fig. 2(a). Over a range of small values of f, it exhibits an anomalous behavior in the sense that, unlike common vehicular traffic, V is not a monotonically decreasing function of the density ρ. Instead a relatively sharp crossover can be observed where the speed *increases* with the density. In the usual form of the fundamental diagram (flux versus density) this transition leads to the existence of an inflection point [Fig. 2(b)]. Assuming that the flux in ant-trail model is given by the equation (6) with a an effective hopping probability $q_{\rm eff}(\rho)$, which depends on the ant density ρ, we can extract $q_{\rm eff}(\rho)$ by fitting the observed flux with $F_{NS}(\rho)$, i.e., from

$$q_{\rm eff}=\frac{F(1-F)}{\rho(1-\rho)}. \tag{7}$$

The effective hopping probability $q_{\rm eff}$ is plotted as a function of ρ for several different values of the parameter f in Fig. 2(c). In the limit $\rho\to 0$, the pheromone dropped by an ant gets enough time to completely evaporate before the following ant comes close enough to smell it; therefore, the ants' hopping probability is almost always q. On the other hand, in the opposite limit $\rho\to 1$, the ants are too close to miss the smell of the pheromone dropped by the leading ant unless the pheromone evaporation probability is very high; consequently, in the limit the ants hop most often with the probability Q.

A proper theory of the ant-trail model should reproduce the nonmonotonic variation of the average speed with density [shown in Fig. 2(a)] and, hence, the unusual shape of the fundamental diagram [shown in Fig. 2(b)]. In this paper, we develope theories, which, indeed, reproduce these features.

B. Models with coupled dynamical variables

Models with coupled dynamical variables have been considered earlier, for example, in the context of reaction-controlled diffusion [19]. However, in this section, we compare the ant-trail model with some more closely related models where the movement of the particles is totally asymmetric.

In the ant-trail model developed in Ref. [20] the particles, which represent the ants, move in a ''ground-potential landscape'' created by the pheromones. A similar approach has also been used for studying the human trails of pedestrians [20].

In the CA model introduced in Ref. [21], for pedestrian dynamics, the floor fields, albeit *virtual*, are analogs of the pheromone fields $\{\sigma\}$ in the ant-trail model. However, these floor fields are ''bosonic'' in the sense that the variable σ, which is by definition non-negative, has an otherwise unrestricted range. In contrast, in our ant-trail model the pheromone field is ''fermionic'' as the variable σ, representing pheromones, can take only two values, namely, 0 (absence) and 1 (presence).

The ant-trail model we propose here is closely related to the bus-route model [22] with parallel updating [23]. In fact, as we will argue now, the ant-trail model and the bus-route model are the two opposite limits of the same generalized version of the NS model of vehicular traffic. The ants are the analogs of the buses while the cells accomodating ants in the ant-trail model are analogs of the bus stops in the bus-route model. Both the models involve two dynamical variables; the variables S and σ in the ant-trail model are the analogs of the variables representing the presence (or absence) of bus and passengers, respectively, in the bus-route model. Just as the number of buses is conserved in the bus-route model, the number of ants is also conserved in our ant-trail model. Similarly, the dynamical variable representing the presence (or absence) of pheromone is not conserved in the ant-trail model just as the number of passangers is not conserved by the dynamics of the bus-route model. However, there is a crucial difference between these two models; in the bus-route model $Q<q$ (as the buses must *slow down* to pick up the waiting passengers) whereas in our ant-trail model $Q>q$ (because an ant is more likely to move forward if it smells pheromone ahead of it). In addition, the pheromone are *dropped* by ants (whereas passengers arrive at the bus stops independent of the buses), while passengers are *picked up* by buses (whereas pheromones evaporate independently).

IV. CLUSTER APPROXIMATION

The simulation results indicate that correlations between different ants as well as between ants and pheromone play an important role. We, therefore, develop a microscopic ''$(2+1)$''-cluster approximation [8,18,24] that allows the inclusion of correlations between the occupation variables $S_{j-1}(t)$ and $S_j(t)$ of two successive sites $j-1$ and j (corresponds to ''2'') and that between the variables $S_j(t)$ and $\sigma_j(t)$ at the same site j (corresponds to ''1'') in an exact way.

The central quantities of the $(2+1)$-cluster approximation are the eight variables

$$P(S_{j-1}(t)S_j(t)), \quad P\begin{pmatrix} S_j(t) \\ \sigma_j(t) \end{pmatrix}, \tag{8}$$

corresponding to all possibilities $[S_{j-1}(t),S_j(t),\sigma_j(t) \in \{0,1\}]$ of finding the corresponding configurations of S and σ at a time. In Appendix A, we will show how the master equation for these quantities can be derived from microscopic considerations and how the resulting equations can be solved consistently.

The flux is given by

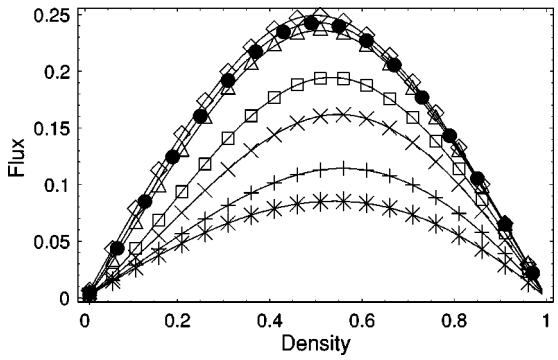

FIG. 3. Fundamental diagrams in the $(2+1)$-cluster approximation. The hopping probabilities are $Q=0.75$ and $q=0.25$. The same symbols in Fig. 2 and in this figure correspond to the same values of f.

$$F=q_{\text{eff}}P(10). \tag{9}$$

In Appendix A, it is shown that within the $(2+1)$-cluster approximation considered here, F can be obtained from the solution of the cubic equation

$$F^2-F+\rho(1-\rho)\left\{q+\frac{(Q-q)(1-f)F}{(1-\rho)f+(1-f)F}\right\}=0. \tag{10}$$

The result is shown in Fig. 3. For all values of f in the range $0<f<1$, the peak of the flux appears at $\rho>1/2$, in qualitative agreement with the general trend observed in Fig. 2. But, this $(2+1)$-cluster approximation cannot reproduce the sharp rise in the fluxes observed in Fig. 2. Note that in each of the three cases $Q=q$, $f=0$, and $f=1$, the solution of Eq. (10) is identical to Eq. (6) with either $q_{NS}=q$ or $q_{NS}=Q$. Next, let us define $P(m)$ as the probability of finding m-size cluster of *ants* in a stationary state. Here the 1-size cluster is defined by $\cdots 010\cdots$, and a m-size cluster consists of a string of m of 1 between 0s. The distribution of cluster sizes is then given by (see Appendix A)

$$P(m)=\frac{P(10)}{\rho}\,\frac{(1-P(10)/\rho)^{m-1}}{1-(1-P(10)/\rho)^{\rho L}}. \tag{11}$$

In Fig. 4, we illustrate the graphs of $P(m)$ given by Eq. (11) and corresponding numerical data. There is a sharp peak at $m=1$ at all the densities and the distributions are exponential. This means that large clusters of ants are rarely seen in this model. Moreover, Eq. (11) fits well with the numerical data for all $\rho>0.5$, but it underestimates the simulations data at lower densities.

In order to get a better understanding of the microscopic structure of the stationary state, we also calculate the probabilities of finding an ant P_a, pheromone P_p, and nothing P_0 in front of an ant:

$$P_a=1-\frac{P(10)}{\rho}, \tag{12}$$

$$P_p=\frac{P(10)}{\rho(1-\rho)}P\begin{pmatrix} 0 \\ 1 \end{pmatrix}, \tag{13}$$

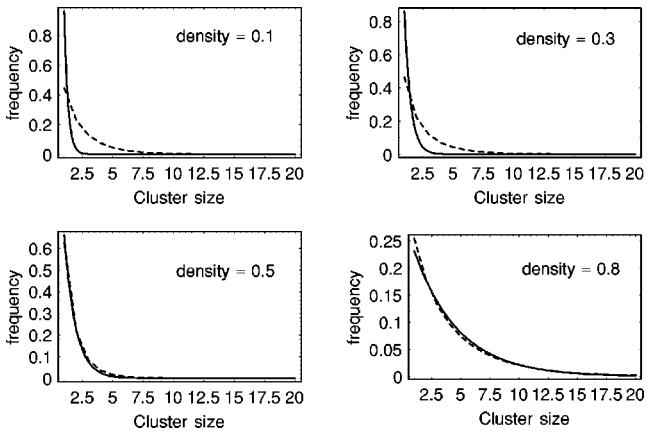

FIG. 4. Cluster-size distribution for $\rho=0.1, 0.3, 0.5,$ and 0.8. Theoretical curve (solid line) given by Eq. (11) underestimates the simulation (broken curve) at densities $\rho<0.5$. Other relevant parameters are $Q=0.75$, $q=0.25$, and $f=0.005$.

$$P_0=\frac{1}{\rho}P(10)-\frac{P(10)}{\rho(1-\rho)}P\begin{pmatrix}0\\1\end{pmatrix}. \tag{14}$$

Note that the sum of these three probabilities is 1. The results are shown in Fig. 5. We see that only for small and large values of f (e.g., $f=0.0001$ and $f>0.1$), the results of the $(2+1)$-cluster approximation are in good quantitative agreement with the corresponding numerical results.

The results derived in this section indicate that the *microscopic* cluster approximation is not able to capture the correlations which lead to the sharp crossover observed for small evaporation probabilities f. A systematic extension of this approximation scheme is, in principle, possible and more correlations could be taken into account. However, this approach will become quite cumbersome. In Appendix B, we have also tried to extend the results in this section by using the stochastic cluster approach [25], but the results are not much improved. In the following we, therefore, develope a *phenomenological* mean-field theory that tries to capture the essential effects in a simple way.

V. HOMOGENEOUS MEAN-FIELD THEORY (HMFT)

In this mean-field theory (MFT), let us assume that all the ants move with the mean speed V that depends on the density ρ of the ants as well as on f; although, to begin with, the nature of these dependences are not known we will obtain these self-consistently. Unlike the usual approach of 1-cluster MFT (i.e., factorization of the probabilities of configurations in terms of 1-cluster probabilities), the HMFT is a *self-consistent* MFT that, as we demonstrate later in this paper, succeeds in capturing part of the correlations, albeit in a heuristic manner.

Let us consider a pair of ants having a gap of n sites in between. We designate the leading ant of this pair as the lead ant (LA) and the other as the following ant (FA). The probability that the site immediately in front of the FA contains pheromone is $(1-f)^{n/V}$. Here n/V is just the average time passed since the LA has dropped the pheromone. Therefore,

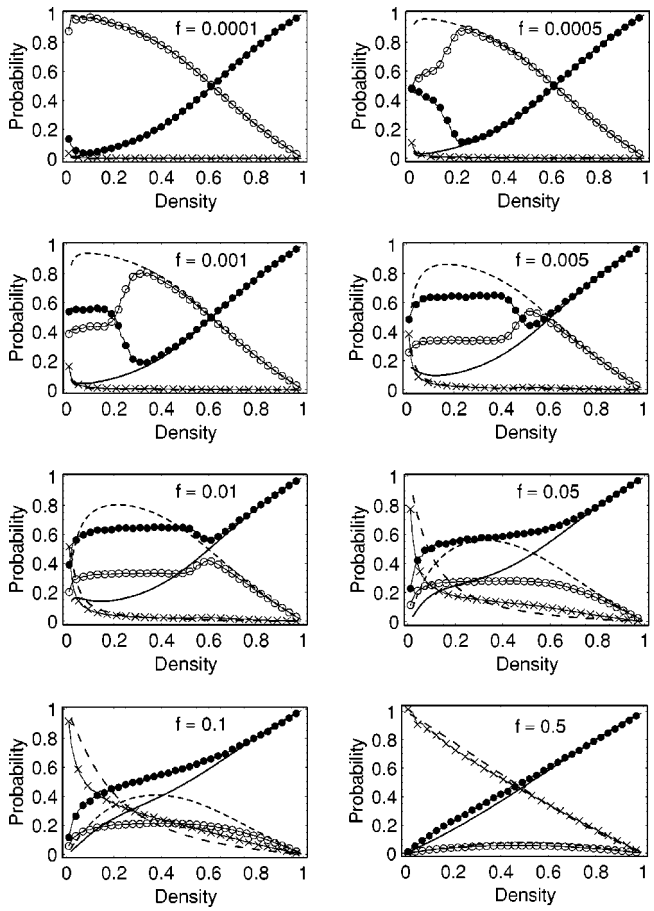

FIG. 5. Probability of finding an ant (solid curve), pheromone (fine broken curve), and nothing (coarse broken curve) in front of an ant, with parameters $f=0.0001, \ldots, 0.5$, in the $(2+1)$-cluster approximation. Numerical data, obtained from computer simulations, are also plotted [ants (●), pheromone but no ant (○), and nothing (×)]. These figures demonstrate how the predictions of the $(2+1)$-cluster approximation deviate from simulation data.

in this zeroth level MFT, the effective hopping probability is given by

$$\eta_0=Q(1-f)^{n/V}+q\{1-(1-f)^{n/V}\}. \tag{15}$$

In the mean-field approximation, we replace n by the corresponding exact global mean separation $\langle n\rangle=(1/\rho)-1$ between successive ants, i.e., we are assuming the existence of a *homogeneous* state. Moreover, since $V_{\max}=1$ the average speed V is identical to the effective hopping probability, and we get the equation

$$\left(\frac{\eta_0-q}{Q-q}\right)^{\eta_0}=(1-f)^{1/\rho-1}, \tag{16}$$

which is to be solved self-consistently for getting η_0 as a function of ρ for a given f.

Before solving Eq. (16) numerically, note that this equation implies that, for *given* f, $\lim_{\rho\to 0}\eta_0=q$; this reflects the fact that, in the low-density regime, the pheromone dropped by an ant gets enough time to completely evaporate before

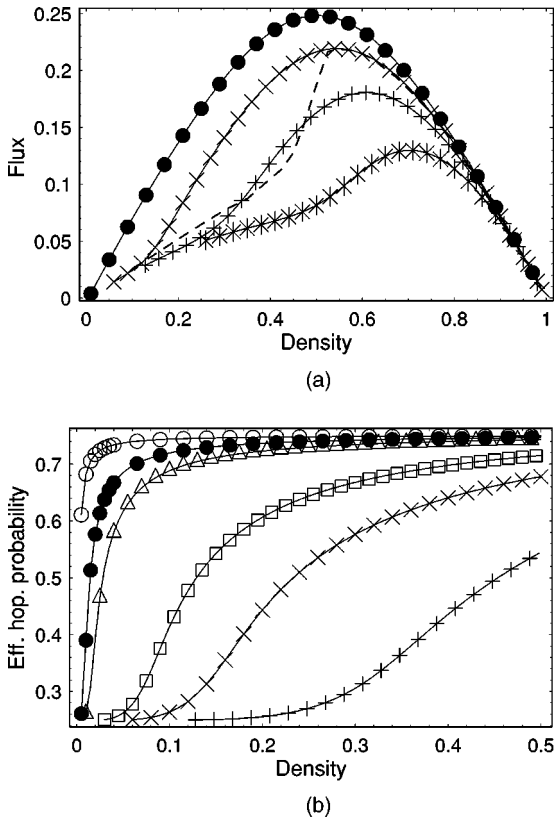

FIG. 6. The fundamental diagram, obtained in the HMFT, is plotted against density in (a) while the corresponding effective hopping probability η_0 is shown in (b). The predictions of the HMFT are shown by the continuous curves; the same symbols in Figs. 2 and 6 correspond to the same values of *f*. The broken curve in (a), corresponding to the computer simulation data for $f=0.005$ taken from Fig. 2(a), highlights the limitations of the HMFT in making *quantitatively* accurate predictions.

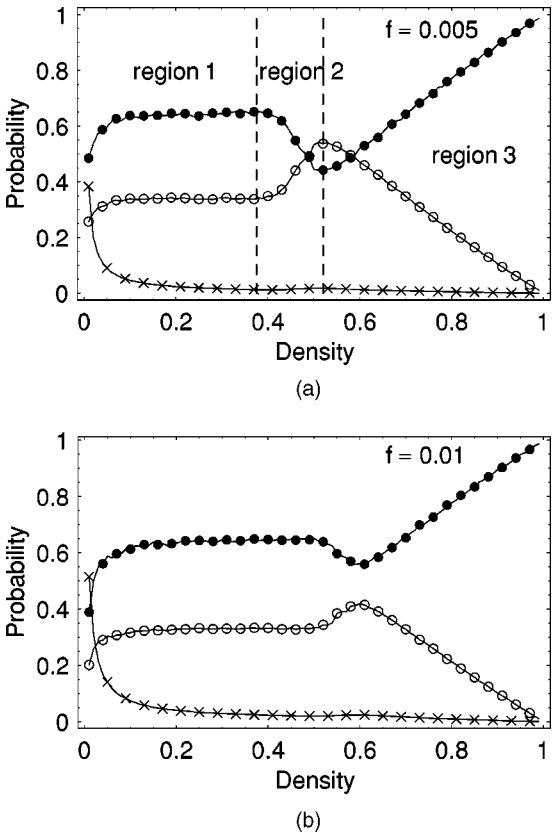

FIG. 7. Numerical results for the probabilities of finding an ant (●), pheromone but no ant (○), and nothing (×) in front of an ant are plotted against the density of the ants. The parameters are $f=0.005$ [in (a)] and $f=0.01$ [in (b)]. See also Fig. 5.

the FA comes close enough to smell it. Equation (16) also implies that $\lim_{\rho\to 1}\eta_0=Q$; this captures the sufficiently high density situations where the ants are too close to miss the smell of the pheromone dropped by the LA unless the pheromone evaporation probability *f* is very high. Similarly, from Eq. (16), we get, for *given* ρ, $\lim_{f\to 1}\eta_0=q$ and $\lim_{f\to 0}\eta_0=Q$, which are also consistent with intuitive expectations.

The solutions of Eq. (16), calculated numerically by using Newton method, are plotted in Fig. 6(b) and the corresponding fundamental diagram is shown in Fig. 6(a). Clearly, the HMFT captures the *qualitative* features of the ant-trail model. However, there are significant *quantitative* differences between the predictions of this theory and the computer simulation data, especially, the sharp crossover around $\rho=0.5$ (Fig. 2). One possible reason is that the HMFT assumes a rather homogeneous stationary state. Therefore, in the following section, we will develope an approximation scheme that emphasizes the formation of a special kind of cluster in the steady state.

VI. "LOOSE" CLUSTER APPROXIMATION (LCA)

Let us consider again the probabilities P_a, P_p, and P_0, defined in the preceding section. For the purpose of clarifying some subtle concepts of "clustering," we replot these probabilities for only two specific values of *f* in Fig. 7; these data have been obtained from computer simulations of our ant-trail model.

There is a flat part of the curves in Fig. 7 in the low-density regime; from now onwards, we shall refer to this region as "region 1." Note that in this region, in spite of low density of the ants, the probability of finding an ant in front of another is quite high. This implies the fact that ants tend to form a cluster. On the other hand, cluster-size distribution (Fig. 4), obtained from our computer simulations, shows that the probability of finding isolated ants are always higher than that of finding a cluster of ants occupying nearest-neighbor sites.

These two apparently contradictory observations can be reconciled by assuming that the ants form loose clusters in the region 1. The term loose means that there are small gaps in between successive ants in the cluster, and the cluster looks like an usual compact cluster if it is seen from a distance (Fig. 8). In other words, a loose cluster is just a loose assembly of isolated ants. Thus it corresponds to a space region with density larger than the average density ρ, but smaller than the maximal density ($\rho=1$) of a compact cluster.

Let us assume that the loose cluster becomes stationary after sufficient time has passed. Then the hopping probability

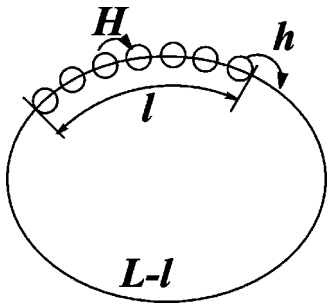

FIG. 8. Schematic explanation of the loose cluster. H is the hopping probability of ants inside the loose cluster and h is that of the leading ant.

of all the ants, except the leading one, is assumed to be H, while that of the leading one is h (see Fig. 8); the values of H and h are determined self-consistently, just as the effective hopping probability in the HMFT was estimated self-consistently in Sec. V. Before beginning the detailed analysis, let us consider the properties of H and h. If f is small enough, then H will be close to Q because the gap between ants is quite small. On the other hand, if the density of ants is low enough, then h will be very close to q because the pheromone dropped by the leading ant would evaporate when the following ant arrives there.

Next we determine the typical size of the gap between successive ants in the cluster. We will estimate this by considering a simple time evolution beginning with an usual compact cluster (with local density $\rho=1$) without any gap in between the ants. Then the leading ant will move forward by one site over the time interval $1/h$. This hopping occurs repeatedly and in the interval of the successive hopping, the number of the following ants that will move one step is H/h. Thus, in the stationary state, strings (compact clusters) of length H/h, separated from each other by one vacant site, will produced repeatedly by the ants (see Fig. 9). Then the average gap between ants is

$$\frac{[(H/h)-1]\times 0+1\times 1}{H/h}=\frac{h}{H}, \tag{17}$$

which is independent of the density ρ of ants. Interestingly, the density-independent average gap in the LCA is consistent with the flat part (i.e., region 1) observed in computer simulations (Fig. 7). In other words, the region 1 is dominated by loose clusters.

Beyond region 1, the effect of pheromone of the last ant becomes dominant. Then the hopping probability of leading ants becomes large and the gap becomes wider, which will increase the flow. We call this region as region 2, in which the looser cluster is formed in the stationary state. It can be characterized by a negative gradient of the density dependence of the probability to find an ant in front of a cell occupied by an ant (see Fig. 7).

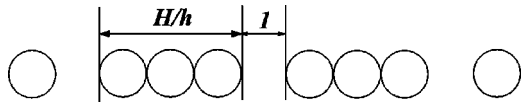

FIG. 9. The stationary loose cluster. The average gap between ants becomes h/H, which is irrelevant to the density of ants.

Considering these facts, we finally obtain the following equations for h and H:

$$\left(\frac{h-q}{Q-q}\right)^h=(1-f)^{L-l},\ \left(\frac{H-q}{Q-q}\right)^H=(1-f)^{h/H}, \tag{18}$$

where l is the length of the cluster given by

$$l=\rho L+(\rho L-1)\frac{h}{H}, \tag{19}$$

and ρ and L are density and the system size, respectively. These equations can be applied to the region 1 and 2, and solved simultaneously by the Newton method.

Total flux in this system is then calculated as follows. The effective density ρ_{eff} in the loose cluster is given by

$$\rho_{\mathrm{eff}}=\frac{1}{1+h/H}. \tag{20}$$

Therefore, considering the fact that there are no ants in the part of the length $L-l$, total flux F is

$$F=\frac{l}{L}f(H,\rho_{\mathrm{eff}}), \tag{21}$$

where $f(H,\rho_{\mathrm{eff}})$ is given by

$$f(H,\rho_{\mathrm{eff}})=\frac{1}{2}(1-\sqrt{1-4H\rho_{\mathrm{eff}}(1-\rho_{\mathrm{eff}})}). \tag{22}$$

Above the density 1/2, ants are assumed to be uniformly distributed, in which a kind of MFT works well. We call this region as region 3. Thus, we have three typical regions in this model. In region 3, the relation $H=h$ holds because all the gaps have the same length, i.e., the state is homogeneous. Thus h is determined by

$$\left(\frac{h-q}{Q-q}\right)^h=(1-f)^{1/\rho-1}, \tag{23}$$

which is the same as our previous paper, and flux is given by $f(h,\rho)$. It is noted that if we put $\rho=1/2$ and $H=h$, then Eq. (18) coincides with Eq. (23).

We can focus on the region 1 by assuming $h=q$ in Eq. (18). Under this assumption, we can easily see that the flux-density relation becomes linear. In Fig. 10(a), the two theoretical lines are almost the same, and the gradient of numerical results are also similar among these values of f, which is quite similar to the theoretical one. In Fig. 10(b), the results obtained from Eq. (18) in the region $\rho\leqslant 1/2$ are shown. Above this value of density, Eq. (23) is used. The jointed curve fits quite well the numerical one.

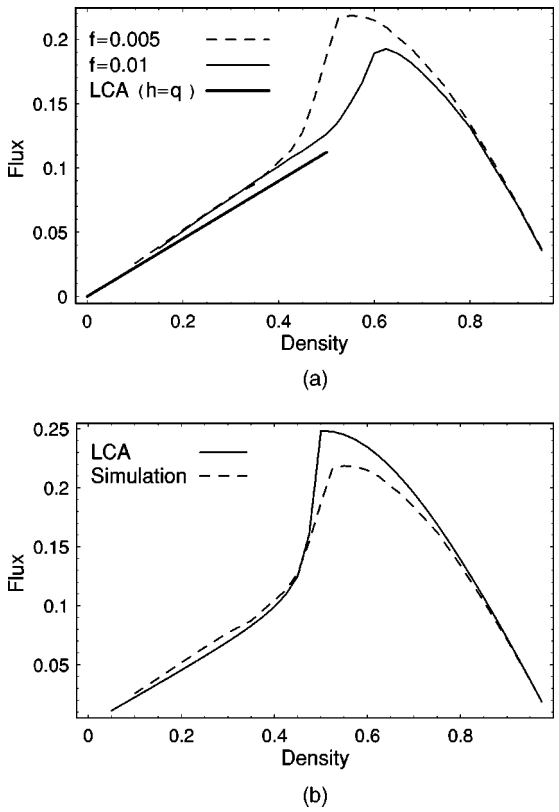

FIG. 10. (a) Fundamental diagrams of the linear region (bold line) together with numerical results with parameters $f=0.005$ (broken curve) and $f=0.01$ (solid curve). (b) The fundamental diagram ($f=0.005$) of the combination of LCA and Eq. (23) (solid curve). The broken curve is the numerical result for $f=0.005$. The system size is $L=350$.

VII. ANT-TRAIL MODEL WITH RANDOM-SEQUENTIAL UPDATING

In our earlier published work [12] as well as in this paper, so far we have considered only parallel updating of the states of the model system. However, in some models different updating schemes are known to give rise to nontrivial differences. For example, the correlations observed in the NS model [17] with parallel dynamics and $V_{\max}=1$ totally disappear when the parallel updating scheme is replaced by random sequential updating. In contrast, the updating scheme does not make much of difference in the bus-route model [22,23]. Therefore, in this section, we examine the effects of replacing the parallel updating by random sequential updating, particularly on the unusual features of the fundamental diagram.

In the ant-trail model with random sequential updating, the updating of the system is done the following way:

(1) A site is choosen randomly.

(2a) If there is no ant, but a pheromone, at the chosen site this is allowed to evaporate with probability f.

(2b) On the other hand, if there is an ant at the chosen site, the usual motion update is done (i.e., it cannot move forward if the site in front is occupied by another ant; otherwise, it moves forward with probability Q or q depending on whether the site in front contains or does not contain pheromone).

(3) If the ant at the randomly chosen site moves forward, a pheromone is created at the new site without making any attempt to let the pheromone left behind in its old position (i.e., at the randomly chosen site) to evaporate.

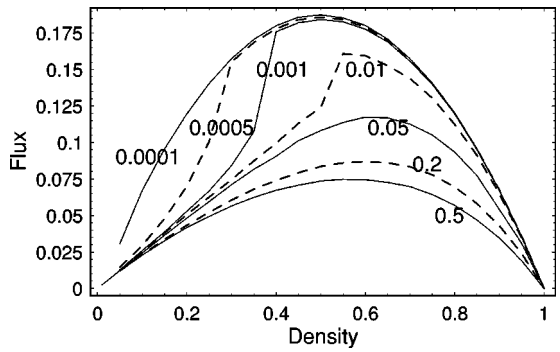

FIG. 11. The flux of the ants, in the ant-trail model with *random sequential updating*, plotted against their densities for the parameters $Q=0.75$ and $q=0.25$.

The flux of the ants in this model is plotted against their density in Fig. 11; the qualitative features of the curves, including the sharp crossover from free to congested state, are similar to those in the original version of this model with parallel updating. From these observations we conclude that, unlike the NS model, the correlations responsible for the nonmonotonic variation of the average speed with the density of the ants are not artefacts of the parallel update scheme but genuine nontrivial features of the model.

VIII. CONCLUDING DISCUSSIONS

A stochastic cellular automaton model of an ant trail, which we have proposed recently [12], has been investigated in detail, both analytically as well as numerically, in this paper. The model is characterized by two coupled dynamical variables, representing the ants and the pheromone. The coupling leads to surprising results, especially an anomalous fundamental diagram. This anomalous shape of the fundamental diagram is a consequence of the nonmonotonic variation of the average speed of the ants with their density in an intermediate range of the rate of pheromone evaporation. These unusual features of the ant-trail model have been analyzed in this paper using various analytical approaches and computer simulations.

It is shown that the homogeneous mean-field approximations are able to capture some of the qualitative features observed in the computer simulations. However, these approximations cannot account for the quantitative data. Therefore, we have analyzed the spatiotemporal organization of the ants and pheromone in the stationary state. This provided some insights, which we have utilized to develope a different scheme of calculations that we call loose-cluster approximation.

By studying appropriate correlation functions, we were able to distinguish three different regimes of density. At low densities (region 1), the behavior is dominated by the exis-

tence of loose clusters that are formed through the interplay between the dynamics of ants and pheromone. In region 2, occuring at intermediate densities, the enhancement of the hopping probability due to pheromone is dominant. Finally, in region 3, at large densities the mutual hindrance against the movements of the ants dominates the flow behavior leading to a homogeneous state similar to that of the NS model.

We have seen that the observed effects persist for random sequential updating. For this case, we also expect that exact results can be achieved by using the matrix-product technique [4,26]. Extensions of this model, including counterflow and random sequential dynamics, will be reported in the future.

ACKNOWLEDGMENT

This work was supported in part by the Alexander von Humboldt Foundation (D.C.).

APPENDIX A: (2+1)-CLUSTER APPROXIMATION

In this appendix, we provide details for the (2+1)-cluster approximation scheme developed in Sec. IV. There we have introduced the eight dynamical variables, Eq. (8), which allow to take into account correlations between occupation numbers of consecutive sites and between occupation numbers of ants and pheromone.

These variables are not independent. Instead, we can immediately write down the following six equations:

$$P(10)=P(01), \tag{A1}$$

$$P\begin{pmatrix}1\\0\end{pmatrix}=0, \tag{A2}$$

$$P(00)+P(01)+P(10)+P(11)=1, \tag{A3}$$

$$P\begin{pmatrix}0\\0\end{pmatrix}+P\begin{pmatrix}0\\1\end{pmatrix}+P\begin{pmatrix}1\\0\end{pmatrix}+P\begin{pmatrix}1\\1\end{pmatrix}=1, \tag{A4}$$

$$P(00)+P(10)=1-\rho, \tag{A5}$$

$$P\begin{pmatrix}0\\0\end{pmatrix}+P\begin{pmatrix}0\\1\end{pmatrix}=1-\rho, \tag{A6}$$

where ρ is the ant density. Equation (A1) expresses the particle-hole symmetry condition while the Eq. (A2) is a consequence of the definition of the model. The other equations are known as Kolmogorov consistency conditions [24].

We need two more equations in order to obtain the expression for all the eight variables in Eq. (8). These are obtained by considering the master equations for, say, $P(00)$ and $P\binom{0}{1}$. In the $(2+1)$-cluster approximation, the master equation for $P(00)$ is given by

$$\begin{aligned}\overline{P}(00)=&\frac{P(00)}{P(00)+P(10)}P(00)\\&+\frac{P(10)}{P(00)+P(10)}(1-q_{\mathrm{eff}})P(00)\\&+\frac{P(00)}{P(00)+P(10)}P(01)\frac{P(10)}{P(10)+P(11)}q_{\mathrm{eff}}\\&+\frac{P(10)}{P(00)+P(10)}(1-q_{\mathrm{eff}})\\&\times P(01)\frac{P(10)}{P(10)+P(11)}q_{\mathrm{eff}},\end{aligned} \tag{A7}$$

where $\overline{P}(00)$ is $P(00)$ of the next time step, i.e., at the time step $t+1$, while the probabilities on the right-hand side refer to the time step t. The four terms in the right-hand side rhs of Eq. (A7) comprise all the configurations and processes that give rise to the configuration $(S_{j-1}S_j)=(00)$ in the next time step. Here we put $\overline{P}(00)=P(00)$ in Eq. (A7) in order to obtain the stationary solution for $P(00)$. Then we have

$$P(00)=\frac{(1-q_{\mathrm{eff}})P(10)^2}{\rho-P(10)}. \tag{A8}$$

Thus substituting Eq. (A8) into Eq. (A5) using Eq. (9), we obtain

$$F^2-F+q_{\mathrm{eff}}\rho(1-\rho)=0. \tag{A9}$$

Similarly, the master equation for $P\binom{0}{1}$ is given by

$$\begin{aligned}\overline{P}\begin{pmatrix}0\\1\end{pmatrix}=&\frac{P(00)}{P(00)+P(10)}P\begin{pmatrix}0\\1\end{pmatrix}(1-f)\\&+\frac{P(10)}{P(00)+P(10)}P\begin{pmatrix}0\\1\end{pmatrix}(1-q_{\mathrm{eff}})(1-f)\\&+P\begin{pmatrix}1\\1\end{pmatrix}\frac{q_{\mathrm{eff}}P(10)}{P(10)+P(11)}(1-f).\end{aligned} \tag{A10}$$

Using $P\binom{1}{1}=\rho$, we obtain the stationary solution from Eq. (A10) as

$$P\begin{pmatrix}0\\1\end{pmatrix}=\frac{(1-f)F}{f+\dfrac{1-f}{1-\rho}F}, \tag{A11}$$

where we use the relation

$$F=q_{\mathrm{eff}}P(10)=P(10)\frac{qP\begin{pmatrix}0\\0\end{pmatrix}+QP\begin{pmatrix}0\\1\end{pmatrix}}{P\begin{pmatrix}0\\0\end{pmatrix}+P\begin{pmatrix}0\\1\end{pmatrix}}. \tag{A12}$$

From Eqs. (A12) and (A11), we have

$$q_{\rm eff}=q+(Q-q)\frac{(1-f)F}{(1-\rho)f+(1-f)F}. \qquad \text{(A13)}$$

Finally, substituting Eq. (A13) into Eq. (A9), we obtain the cubic equation (10) for the flux F.

We can also calculate the distribution of cluster sizes defined in Sec. IV. We can write it as

$$P(m)=\frac{1}{C}P(01)\left(\frac{P(11)}{P(10)+P(11)}\right)^{m-1}\frac{P(10)}{P(10)+P(11)}$$
$$=\frac{1}{C}\frac{P(10)^2}{\rho}\left(1-\frac{P(10)}{\rho}\right)^{m-1}. \qquad \text{(A14)}$$

Here C is determined through the normalization condition $\Sigma_{m=1}^{L}P(m)=1$, where L is the system size, as

$$C=P(10)\left\{1-\left(1-\frac{P(10)}{\rho}\right)^{\rho L}\right\}. \qquad \text{(A15)}$$

Thus $P(m)$ is given by Eq. (11).

Let us also consider the the probability of finding an ant, pheromone, and nothing in the front site discussed in Sec. VI. The probability of finding an ant is simply given by $P(11)$. The probability of finding pheromone without an ant, and that of nothing are given, respectively, by

$$P(10)\frac{P\binom{0}{1}}{P\binom{0}{0}+P\binom{0}{1}},\quad P(10)\frac{P\binom{0}{0}}{P\binom{0}{0}+P\binom{0}{1}}. \qquad \text{(A16)}$$

Normalizing these quantities by dividing ρ, we obtain each probability by only using $P(10)$ and $P\binom{0}{1}$ as given in Eqs. (12)–(14).

APPENDIX B: STOCHASTIC CLUSTER APPROXIMATION

Let us extend the analysis in the Appendix A following the approach used in analyzing the stochastic car cluster model proposed in Ref. [25]. In the model, one cluster of cars is assumed to exist in the background of stationary uniform flow, while in Appendix A we only consider the uniform flow to derive flux of ants, and neglect the clustering effect. The cluster-size distribution $P(m)$ was derived as the stationary solution of its master equation in Ref. [25]. However, since we have already obtained $P(m)$, we will use Eq. (11) instead of considering the master equation. The flux in cluster is considered to be zero, thus total flux in a given configuration of this system is given by $0\times(m-1)/L+F_m\times[1-(m-1)/L]$ if m-size cluster exists. Here F_m represents the uniform flux under the existance of m-size cluster, which is defined by using Eq. (10) as

$$F_m^2-F_m+\rho_m(1-\rho_m)\left\{q+\frac{(Q-q)(1-f)F_m}{(1-\rho_m)f+(1-f)F_m}\right\}=0, \qquad \text{(B1)}$$

and ρ_m is given by

$$\rho_m=\frac{\rho-(m-1)/L}{1-(m-1)/L}. \qquad \text{(B2)}$$

In these equations, we take into account that the density of the uniform flow is reduced due to the existance of m-size cluster.

Thus, the flux of this stochastic cluster approximation is finally given by

$$F(\rho)=\sum_{m=1}^{L}P(m)\left(1-\frac{m-1}{L}\right)F_m. \qquad \text{(B3)}$$

Note that if only the first term on the rhs of Eq. (B3) is retained and all the other terms are dropped, the expression for $F(\rho)$ reduces to the the fundamental diagrams obtained in the $(2+1)$-cluster approximation (and plotted in Fig. 3). We have evaluated Eq. (B3) numerically by using the distribution (11), but the results are almost the same as Fig. 3 and, therefore, not shown here. This, however, is not surprising in view of the fact that the rhs of Eq. (B3) is dominated by $m=1$ because of the sharp peak of $P(m)$ at $m=1$.

[1] B. Schmittmann and R.K.P. Zia, in *Phase Transitions and Critical Phenomena*, edited by C. Domb and J.L. Lebowitz (Academic Press, New York, 1995), Vol. 17.

[2] G. Schütz, in *Phase Transitions and Critical Phenomena*, edited by C. Domb and J.L. Lebowitz (Academic Press, New York, 2000), Vol. 19.

[3] *Nonequilibrium Statistical Mechanics in One Dimension*, edited by V. Privman (Cambridge University Press, Cambridge, 1997).

[4] B. Derrida, Phys. Rep. **301**, 65 (1998).

[5] J. Marro and R. Dickman, *Nonequilibrium Phase Transitions in Lattice Models* (Cambridge University Press, Cambridge, 1999).

[6] B. Chopard and M. Droz, *Cellular Automata Modelling of Physical Systems* (Cambridge University Press, Cambridge, 1998).

[7] S. Wolfram, *Theory and Applications of Cellular Automata* (World Scientific, Singapore, 1986); *Cellular Automata and Complexity* (Addison-Wesley, Reading, MA, 1994).

[8] D. Chowdhury, L. Santen, and A. Schadschneider, Phys. Rep. **329**, 199 (2000); A. Schadschneider, Physica A **313**, 153 (2002).

[9] D. Helbing, Rev. Mod. Phys. **73**, 1067 (2001).

[10] T. Nagatani, Rep. Prog. Phys. **65**, 1331 (2002).

[11] *Traffic and Granular Flow*, edited by D.E. Wolf, M. Schreckenberg, and A. Bachem (World Scientific, Singapore, 1996); *Traffic and Granular Flow'97*, edited by M. Schreckenberg and D.E. Wolf (Springer, Singapore, 1998); *Traffic and Granular Flow '99*, edited by D. Helbing, H.J. Herrmann, M. Schreckenberg, and D.E. Wolf (Springer, Berlin, 2000).

[12] D. Chowdhury, V. Guttal, K. Nishinari, and A. Schadschneider, J. Phys. A **35**, L573 (2002).

[13] M. Burd, D. Archer, N. Aranwela, and D.J. Stradling, Am. Nat. **159**, 283 (2002).
[14] E.O. Wilson, *The Insect Societies* (Belknap, Cambridge, 1971); B. Hölldobler and E.O. Wilson, *The Ants* (Belknap, Cambridge, 1990).
[15] S. Camazine, J.L. Deneubourg, N.R. Franks, J. Sneyd, G. Theraulaz, and E. Bonabeau, *Self-Organization in Biological Systems* (Princeton University Press, Princeton, 2001).
[16] A.S. Mikhailov and V. Calenbuhr, *From Cells to Societies* (Springer, Berlin, 2002).
[17] K. Nagel and M. Schreckenberg, J. Phys. I **2**, 2221 (1992).
[18] M. Schreckenberg, A. Schadschneider, K. Nagel, and N. Ito, Phys. Rev. E **51**, 2939 (1995); A. Schadschneider and M. Schreckenberg, J. Phys. A **26**, L679 (1993); A. Schadschneider, Eur. Phys. J. B **10**, 573 (1999).
[19] S. Trimper, U.C. Täuber, and G. Schütz, Phys. Rev. E **62**, 6071 (2000).
[20] D. Helbing, F. Schweitzer, J. Keltsch, and P. Molnar, Phys. Rev. E **56**, 2527 (1997); see also Ref. [9].
[21] C. Burstedde, K. Klauck, A. Schadschneider, and J. Zittartz, Physica A **295**, 507 (2001).
[22] O.J. O'Loan, M.R. Evans, and M.E. Cates, Phys. Rev. E **58**, 1404 (1998).
[23] D. Chowdhury and R.C. Desai, Eur. Phys. J. B **15**, 375 (2000).
[24] H.A. Gutowitz, J.D. Victor, and B.W. Knight, Physica D **28**, 18 (1987).
[25] R. Mahnke and J. Kaupuzs, Netw. Spatial Econ. **1**, 103 (2001).
[26] B. Derrida and M.R. Evans, in *Nonequilibrium Statistical Mechanics in One Dimension*, edited by V. Privman (Cambridge University Press, Cambridge, 1997).